

Article

Catalytic Hydrogenation and Dehydrogenation Reactions of *N*-alkyl-bis(carbazole)-Based Hydrogen Storage Materials

Joori Jung ^{1,2,†}, Byeong Soo Shin ^{3,4,†}, Jeong Won Kang ^{4,5,*} and Won-Sik Han ^{1,*} ¹ Department of Chemistry, Seoul Women's University, Seoul 01797, Korea; wydos0312@naver.com² REYON Pharmaceutical, Co., Ltd., Anyang 01459, Korea³ Hyundai Motor Company, Strategy & Technology Division, Ulwang 16082, Korea; bss@hyundai.co.kr⁴ Department of Chemical and Biological Engineering, Korea University, Seoul 02841, Korea⁵ Graduate School of Energy and Environment, Korea University, Seoul 02841, Korea

* Correspondence: jwkang@korea.ac.kr (J.W.K.); wshan@swu.ac.kr (W.-S.H.)

† These authors contributed equally.

Abstract: Recently, there have been numerous efforts to develop hydrogen-rich organic materials because hydrogen energy is emerging as a renewable energy source. In this regard, we designed and prepared four new materials based on *N*-alkyl-bis(carbazole), 9,9'-(2-methylpropane-1,3-diyl)bis(9*H*-carbazole) (**MBC**), 9,9'-(2-ethylpropane-1,3-diyl)bis(9*H*-carbazole) (**EBC**), 9,9'-(2-propylpropane-1,3-diyl)bis(9*H*-carbazole) (**PBC**), and 9,9'-(2-butylpropane-1,3-diyl)bis(9*H*-carbazole) (**BBC**), to investigate their hydrogen adsorption/hydrogen desorption reactivity depending on the length of the alkyl chain. The gravimetric densities of **MBC**, **EBC**, **PBC**, and **BBC** were 5.86, 5.76, 5.49, and 5.31 H₂ wt %, respectively, again depending on the alkyl chain length. All materials showed complete hydrogenation reactions under ruthenium on an alumina catalyst at 190 °C, and complete reverse reactions and dehydrogenation reactions were observed under palladium on an alumina catalyst at <280 °C. At this temperature, all the prepared compounds were thermally stable, and no decomposition was observed.

Keywords: hydrogen storage; carbazole; catalytic hydrogenation/dehydrogenation



Citation: Jung, J.; Shin, B.S.; Kang, J.W.; Han, W.-S. Catalytic Hydrogenation and Dehydrogenation Reactions of *N*-alkyl-bis(carbazole)-Based Hydrogen Storage Materials. *Catalysts* **2021**, *11*, 123. <https://doi.org/10.3390/catal11010123>

Received: 21 December 2020

Accepted: 13 January 2021

Published: 15 January 2021

Publisher's Note: MDPI stays neutral with regard to jurisdictional claims in published maps and institutional affiliations.



Copyright: © 2021 by the authors. Licensee MDPI, Basel, Switzerland. This article is an open access article distributed under the terms and conditions of the Creative Commons Attribution (CC BY) license (<https://creativecommons.org/licenses/by/4.0/>).

1. Introduction

Research on renewable energy has received considerable attention owing to fossil fuel depletion and global warming. Some renewable energies include hydrogen, wind power, hydropower, geothermal energy, bioenergy, and solar energy. Among them, hydrogen energy is the most promising alternative to replace fossil fuels because of its abundant reserves, extensive sources, and high energy density [1–4].

Hydrogen storage methods can be classified into physical and chemical methods. Physical methods include use of high-pressure tanks [5] or cryogenic environments [6]. A significant amount of hydrogen can be stored in high-pressure storage tanks, similar to the storage of natural gas. However, this method has some disadvantages, such as low volumetric capacity and high compression energy. Meanwhile, although the cryogenic storage method provides a high volumetric capacity, it consumes more energy to maintain cryogenic temperatures, which makes it challenging to apply in practice.

Chemical storage via catalytic hydrogenation of small unsaturated organic molecules has been considered an alternative option [7,8]. Initially, the research was focused on cycloalkane compounds such as cyclohexane [9] and methylcyclohexane [10]. They can act as hydrogen storage materials by using catalytic reaction pairs through the dehydrogenation of cycloalkanes and hydrogenation of corresponding aromatics [11–13]. However, dehydrogenation of cycloalkanes is kinetically and thermodynamically difficult; it requires highly active catalysts and high temperatures. These harsh conditions can lead to undesirable side reactions that can be detrimental to proton exchange membrane fuel cells, which are

critically dependent on the purity of hydrogen gas and the material reversibility for hydrogen storage [8]. To solve this problem, heteroatoms such as nitrogen and oxygen were introduced into aromatic molecules. With this strategy, dehydrogenation enthalpy is greatly reduced, and hydrogen can be released in a relatively suitable temperature range [14,15]. To date, *N*-ethylcarbazole (NEC) is one of the most studied materials for small organic compound-based chemical hydrogen storage. It has a high gravimetric density of 5.7 H₂ wt %, and its hydrogenation [16–18] and dehydrogenation [19–26] reactions can proceed under mild conditions without any side reactions. However, the melting point of NEC is 69 °C, which requires additional heat to ensure that the reaction mixture maintains liquid form in real applications. In addition, since the dehydrogenation reaction is an endothermic reaction, a significant amount of heat is required to generate H₂ gas. In this regard, this field of research has recently focused on the integration of fuel cells in the liquid organic hydrogen carrier system [27–29]. Namely, the high-temperature waste heat of fuel cells can be used to heat the dehydrogenation reactor. For example, waste heat generated by solid oxide fuel cell is about 300 °C, which is enough to use for the dehydrogenation reaction. For this application, the storage material should exhibit high thermal stability [30]. Unfortunately, the thermal stability of NEC is insufficient because it decomposes at 180 °C [31]. Therefore, there is a need to find new hydrogen storage materials with high thermal stability.

In this work, four new materials based on *N*-alkyl-bis(carbazole) were designed and prepared to investigate their hydrogen adsorption/hydrogen desorption reactivity depending on the length of the alkyl chains. The synthesis of the designed materials was optimized, and their structural analyses were performed to investigate the structure-property relationship. Detailed thermal properties were analyzed by thermogravimetric analysis (TGA) and differential scanning calorimetry (DSC) measurements, and their hydrogenation/dehydrogenation reactions were examined, which showed that these materials are promising candidate materials for hydrogen storage.

2. Experimental Section

2.1. General Information

All experiments were carried out with nitrogen purge using the Schlenk technique. Tetrahydrofuran (THF) was freshly distilled over sodium and benzophenone. ¹H and ¹³C NMR spectra were recorded on a Bruker Fourier 300 MHz spectrometer operated at 300.1 and 75.4 MHz, respectively. ¹H and ¹³C NMR chemical shifts were measured in CDCl₃ and referenced to the relative peaks of CHCl₃ (7.26 ppm for ¹H NMR) and CDCl₃ (77.16 ppm for ¹³C NMR). Lithium aluminum hydride, diethyl 2-ethyl malonate, diethyl 2-propyl malonate, diethyl 2-butyl malonate, 4-toluenesulfonyl chloride, 2-methyl-1,3-propanediol, carbazole, sodium hydroxide, ruthenium on alumina, and palladium on alumina were purchased from Aldrich or Tokyo Chemical Industry (TCI) and used without further purification. Starting compounds, alkyl diols (**1b–1d**), were prepared by the reduction of carbonyl in the presence of LiAlH₄ as a reducing reagent in high yield [32].

2.2. Synthesis

Alkyl diols (1b–1d) LiAlH₄ (30 mmol) was placed in a two-necked flask under nitrogen atmosphere. Then, THF (150 mL) was added carefully. Alkyl ethylmalonate (20 mmol) was added dropwise at 0 °C. The resulting mixture was stirred at room temperature overnight and then refluxed for an additional 24 h. After cooling to 0 °C, the reaction mixture was quenched with 15% NaOH. Aluminum salt was filtered, and the filtrate was concentrated under reduced pressure using a rotary evaporator. The residue crude product was used for the next step without further purification.

2-Methylpropane-1,3-diyl bis(4-methylbenzenesulfonate) (2a) Pyridine (50 mL), **1a** (20 mmol), and 4-toluenesulfonyl chloride (60 mmol) were stirred under nitrogen atmosphere. The mixture was reacted at room temperature for 16 h. The reaction mixture was quenched with 6 M HCl and extracted with ethyl acetate. The organic layer was evaporated under reduced pressure. The crude product was purified by silica gel column

chromatography using ethyl acetate/*n*-hexane (*v/v* = 1:3) as an eluent. The product was a white solid. Yield: 68%. ¹H NMR (300 MHz, CDCl₃): δ 7.75 (d, 4H, *J* = 6.6 Hz), 7.36 (d, 4H, *J* = 8.1 Hz), 3.94–3.83 (m, 4H), 2.46 (s, 6H), 0.92 (d, 3H, *J* = 7.2 Hz).

2-Ethylpropane-1,3-diyl bis(4-methylbenzenesulfonate) (2b) This compound was prepared using the same procedure as that used for obtaining **2a** except for using **1b** instead of **1a**. Yield: 53%. ¹H NMR (300 MHz, CDCl₃): δ 7.52 (d, 4H, *J* = 6.6 Hz), 7.36 (d, 4H, *J* = 8.1 Hz), 3.96–3.91 (m, 4H), 2.45 (s, 6H), 1.28–1.23 (m, 2H) 0.79 (t, 3H, *J* = 7.53 Hz).

2-Propylpropane-1,3-diyl bis(4-methylbenzenesulfonate) (2c) This compound was prepared using the same procedure as that used for obtaining **2a** except for using **1c** instead of **1a**. Yield: 54%. ¹H NMR (300 MHz, CDCl₃): δ 7.74 (d, 4H, *J* = 6.6 Hz), 7.36 (d, 4H, *J* = 7.8 Hz), 3.98–3.86 (m, 4H), 2.45 (s, 6H), 1.21–1.16 (m, 2H) 0.82 (t, 3H, *J* = 6.9 Hz).

2-Butylpropane-1,3-diyl bis(4-methylbenzenesulfonate) (2d) This compound was prepared using the same procedure as that used for obtaining **2a** except for using **1d** instead of **1a**. Yield: 54%. ¹H NMR (300 MHz, CDCl₃): δ 7.75 (d, 4H, *J* = 6.6 Hz), 7.36 (d, 4H, *J* = 7.8 Hz), 3.98–3.86 (m, 4H), 2.46 (s, 6H), 1.24–1.11 (m, 2H) 0.81 (t, 3H, *J* = 6.9 Hz).

9,9'-(2-Methylpropane-1,3-diyl)bis(9H-carbazole) (MBC) 9H-Carbazole (13.3 mmol), **2a** (6.06 mmol), and NaOH (72.6 mmol) were stirred under nitrogen atmosphere. Acetone/H₂O (*v/v* = 10:1) was then added. The reaction mixture was kept at room temperature for 30 min and was refluxed for 72 h. After cooling to room temperature, the reaction mixture was quenched with water and extracted with dichloromethane. The organic layer was filtered and concentrated under reduced pressure. The mixture was purified by flash column chromatography using dichloromethane/*n*-hexane (*v/v* = 1:1). The product was a white solid. (*R_f* = 0.4). Yield: 60%. ¹H NMR (300 MHz, CDCl₃): δ 8.11 (d, 4H, *J* = 7.2 Hz), 7.38 (t, 4H, *J* = 7.2 Hz), 7.24–7.20 (m, 8H), 4.23 (m, 4H), 3.08 (m, 1H), 1.06 (d, 3H, *J* = 6.6 Hz); ¹³C NMR (MHz, CDCl₃): δ 140.60, 125.86, 122.98, 120.54, 119.17, 108.79, 47.21, 34.57, 17.33. HRMS (FAB) calcd for C₂₈H₂₄N₂ (388.1939); found 388.1942, elemental anal. calcd: C₂₈H₂₄N₂: C, 86.56; H, 6.23; N, 7.21. Found: C, 86.58; H, 6.22; N, 7.20.

9,9'-(2-Ethylpropane-1,3-diyl)bis(9H-carbazole) (EBC) This compound was prepared using the same procedure as that used for obtaining **MBC** except for using **2b** instead of **2a**. Yield: 60% ¹H NMR (300 MHz, CDCl₃): δ 8.11 (d, 4H, *J* = 7.5 Hz), 7.35 (t, 4H, *J* = 8.1 Hz), 7.21 (t, 4H, *J* = 6.9 Hz), 7.09 (d, 4H, *J* = 8.1 Hz) 4.38–4.08 (dq, 4H, *J* = 7.8 Hz), 2.88 (m, 1H), 1.58–1.53 (m, 2H), 1.05 (t, 3H, *J* = 7.5 Hz); ¹³C NMR (MHz, CDCl₃): δ 140.61, 125.86, 122.97, 120.53, 119.14, 108.74, 45.10, 40.50, 24.38, 11.41. HRMS (FAB) calcd for C₂₉H₂₆N₂ (402.2096); found 402.2098, elemental anal. calcd: C₂₉H₂₆N₂: C, 86.53; H, 6.51; N, 6.96. Found: C, 86.56; H, 6.54; N, 6.98.

9,9'-(2-Propylpropane-1,3-diyl)bis(9H-carbazole) (PBC) This compound was prepared using the same procedure as that used for obtaining **MBC** except for using **2c** instead of **2a**. Yield: 47% ¹H NMR (300 MHz, CDCl₃): δ 8.10 (d, 4H, *J* = 7.2 Hz), 7.37 (t, 4H, *J* = 7.2 Hz), 7.23 (t, 4H, *J* = 6.9 Hz), 7.09 (d, 4H, *J* = 8.1 Hz) 4.38 (dq, 4H, *J* = 7.8 Hz), 2.97 (m, 1H), 1.55–1.48 (m, 2H), 0.80 (t, 3H, *J* = 3.0 Hz); ¹³C NMR (MHz, CDCl₃): δ 140.63, 215.86, 122.96, 120.52, 119.13, 108.72, 45.45, 38.91, 33.77, 20.13, 14.43. HRMS (FAB) calcd for C₃₀H₂₈N₂ (416.2252); found 416.2256, elemental anal. calcd: C₃₀H₂₈N₂: C, 86.50; H, 6.78; N, 6.72. Found: C, 86.52; H, 6.76; N, 6.75.

9,9'-(2-Butylpropane-1,3-diyl)bis(9H-carbazole) (BBC) This compound was prepared using the same procedure as that used for obtaining **MBC** except for using **2d** instead of **2a**. Yield: 52% ¹H NMR (300 MHz, CDCl₃): δ 8.09 (d, 4H, *J* = 6.6 Hz), 7.37 (t, 4H, *J* = 6.0 Hz), 7.23 (t, 4H, *J* = 7.8 Hz), 7.08 (d, 4H, *J* = 8.4 Hz) 4.39–4.05 (dq, 4H, *J* = 7.2 Hz), 2.95 (m, 1H), 1.51–1.22 (m, 6H), 0.78 (t, 3H, *J* = 7.2 Hz); ¹³C NMR (MHz, CDCl₃): δ 140.62, 125.84, 122.96, 120.51, 119.12, 108.73, 45.44, 39.04, 31.35, 29.04, 23.06, 14.00. HRMS (FAB) calcd for C₃₁H₃₀N₂ (430.2409); found 430.2411, elemental anal. calcd: C₃₁H₃₀N₂: C, 86.47; H, 7.02; N, 6.51. Found: C, 86.45; H, 7.06; N, 6.54.

2.3. TGA and DSC Measurements

TGA measurements were recorded using a TGA/DSC 1 (Mettler-Toledo Inc., Columbus, Ohio, United States) thermogravimetric analyzer. TGA was conducted several times, and the data were confirmed. The sample was loaded into a weight-tared alumina pan and gated at a rate of 5 °C/min from 25 to 180 °C under flowing nitrogen (50 mL/min). The thermal properties were measured using DSC (Pyris Diamond DSC; Perkin Elmer). A heating rate of 10 °C/min was used to melt the compound, followed by cooling to room temperature at a high cooling rate of 40 °C/min.

2.4. Catalytic Hydrogenation Reaction

Hydrogenation method 1 A mixture of 3.0 g of sample and 0.3 g of ruthenium on alumina (5 wt %) were placed in a batch reactor. Hydrogen gas was purged into the reactor and stabilized for 30 min. The temperature of the stabilized reactor was increased. If the temperature satisfied the condition, the pressure was adjusted to 70 bar to perform the hydrogenation reaction. When the pressure in the reactor decreased, the pressure in the reactor was increased to 70 bar. The reaction was terminated when the pressure of the reactor was no longer reduced.

Hydrogenation method 2 A mixture of 5.0 g of sample and 0.5 g of ruthenium on alumina (5 wt %) were placed in a batch reactor. The reactor was connected to a reference cell, and a hydrogen valve was attached between the reactor and reference cell to control the hydrogen pressure. The hydrogen pressure of the reactor was set to 70 bar, and the reference cell pressure was set to 100 bar in a constant-temperature bath (20 °C). After removing the constant-temperature water bath from the reactor, the reaction temperature was raised to 190 °C. When the pressure decreased below the initial pressure in the reactor, the hydrogen valve was quickly opened to fill the hydrogen gas to the initial pressure from the reference cell. When the reaction reached equilibrium, the reactor was cooled to room temperature. The hydrogen pressure of the reactor was adjusted to a pre-reaction pressure of 70 bar. The yield of the hydrogenation reaction was calculated by the pressure difference.

2.5. Catalytic Dehydrogenation Reaction

Dehydrogenation method (I) Here, 0.11 g of palladium on alumina (5 wt %) catalyst was placed in a 50 mL three-necked round flask. The reactor was purged with nitrogen to remove air. The MFM (mass-flow meter) was run to confirm the stabilization of nitrogen. After raising the temperature to the value required by the reaction, a fully hydrogenated sample was injected into the flask. While monitoring the MFM graph, the reaction was terminated if no more hydrogen gas was released. Dehydrogenation of all fully hydrogenated samples was complete within 2 h. The mixture was characterized by ¹H NMR.

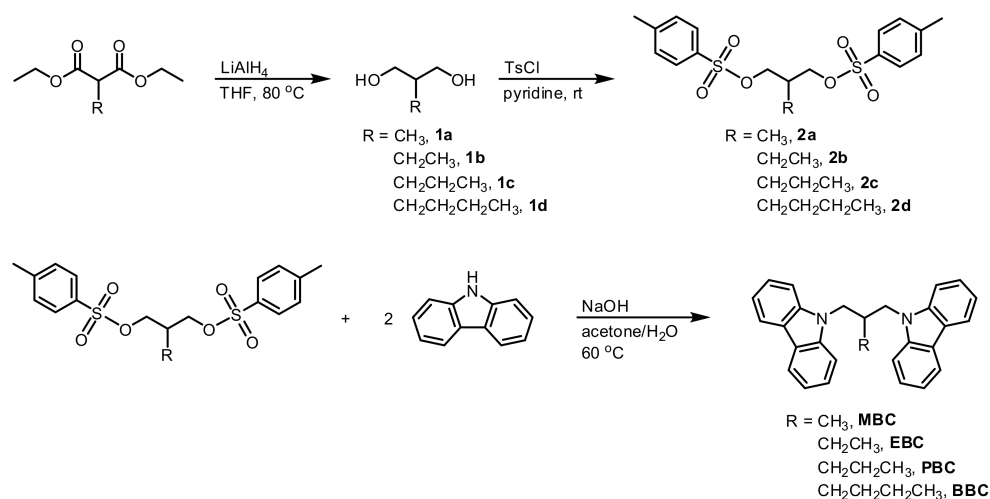
Dehydrogenation method (II) A mixture of 0.2 g of palladium on alumina (5 wt %) and 1.0 g of a fully hydrogenated sample was placed in a 50 mL three-necked round flask. The reactor was purged with nitrogen to remove air. The nitrogen gas valve was closed, and the reaction temperature was increased. The release of hydrogen in the reactor was confirmed by MFM. After 1 h, if no hydrogen was released, the reaction was stopped. The mixture was characterized by ¹H NMR.

3. Results and Discussion

3.1. Synthesis

Scheme 1 shows the synthetic procedure for the designed compounds. Initially, 2-ethyl-1,3-propanediol (**1b**), 2-propyl-1,3-propanediol (**1c**), and 2-butyl-1,3-propanediol (**1d**) were prepared by reducing the starting malonates, diethyl 2-ethyl malonate, diethyl 2-propyl malonate, and diethyl 2-butyl malonate, respectively, as described previously [32]. The resulting intermediate compounds, 2-methylpropane-1,3-diyl-bis(4-methylbenzenesulfonate) (**2a**), 2-ethylpropane-1,3-diyl-bis(4-methylbenzenesulfonate) (**2b**), 2-propylpropane-1,3-diyl-bis(4-methylbenzenesulfonate) (**2c**), and 2-butylpropane-1,3-diyl-bis(4-methylbenzenesulfonate) (**2d**), were prepared by reacting with the corresponding

alkyl diols (**1a–1d**) with 4-toluenesulfonyl chloride in a modest yield. The final products, **MBC**, **EBC**, **PBC**, and **BBC**, were synthesized by the following method: substitution reactions of alkyl tosylates (**2a–2d**) with 9*H*-carbazole were carried out under reflux conditions in a mixed solvent of acetone/water in the presence of sodium hydroxide as a base. After the reaction, the final products were further purified by column chromatography. Structural analysis and purities of the final products were confirmed by ¹H and ¹³C NMR spectroscopy, mass spectroscopy, and elemental analysis (summarized in the Experimental Section).



Scheme 1. Synthetic procedures for **MBC**, **EBC**, **PBC**, and **BBC**.

3.2. Thermal Properties

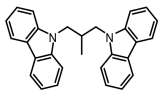
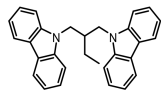
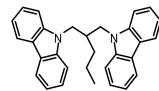
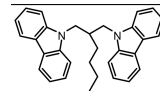
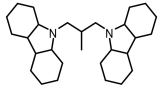
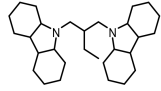
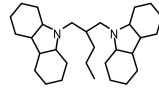
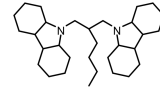
The thermal stabilities of **MBC**, **EBC**, **PBC**, and **BBC** were measured using TGA and DSC, as summarized in Table 1 and the results are shown in Figure 1. The thermal decomposition temperatures (T_d) of **MBC**, **EBC**, **PBC**, and **BBC** were 344, 343, 347, and 364 °C, respectively. As seen, thermal stabilities increased with increasing alkyl chain length, and their higher thermal stabilities compared to that of **NEC** ($T_d = 180$ °C) [31] can be attributed to symmetric geometries and increased molecular weight. It should be noted that the enhanced thermal stability is important for real applications in hydrogen storage systems because the generated thermal heat in the fuel cell is generally higher than 300 °C. Since the thermal stability of all prepared compounds satisfies this requirement, it is expected that these materials can be used in fuel cell systems. The melting points were analyzed by DSC. For this purpose, samples were subjected to a nitrogen gas purge and measured at a heating rate of 10 °C min⁻¹. The melting points of **MBC**, **EBC**, **PBC**, and **BBC** were 154, 187, 200, and 198 °C, respectively, as shown in Figure 1b. The melting points increased rather than decreased as the length of the alkyl chains increased. This phenomenon can be explained by the existence of a plane of symmetry in all prepared compounds and the influence of π - π stacking between carbazole groups. In addition, all compounds might be compacted in the form of spheres due to free rotation, thereby reducing the surface area and increasing the melting point.

3.3. Catalytic Hydrogenation Reactions

For hydrogenation reactions, each compound was added into a batch reactor in the presence of ruthenium on alumina catalyst, and the reaction mixture was heated at a constant temperature of 190 °C for 24 h under a hydrogen pressure of 60–70 bar. The reactions for all compounds were completed within 7 h. Ruthenium on alumina was used as the catalyst because it has been reported that other catalysts produced side products, while ruthenium on alumina resulted in selective reaction without any stereoisomers [19]. After the hydrogenation reactions, the structures of the products **MBC-H**, **EBC-H**, **PBC-H**,

and **BBC-H** were analyzed by ^1H NMR, as shown in Figures S9–S12. For all compounds, the signals between 7 and 8 ppm, attributed to protons in the aromatic rings, completely disappeared, and only aliphatic proton peaks at 0.5–3.0 ppm were observed, indicating that carbazole groups were converted into dodecahydro-carbazole. The gravimetric densities were calculated from the difference in the reference cell pressure when the temperature and pressure were adjusted before and after the hydrogen reactions. As a result, the gravimetric densities of **MBC-H**, **EBC-H**, **PBC-H**, and **BBC-H** were calculated as 5.92 ± 0.24 , 5.81 ± 0.24 , 5.34 ± 0.24 , and 5.61 ± 0.24 H_2 wt %, respectively, as summarized in Table 2.

Table 1. Relevant properties of **MBC**, **EBC**, **PBC**, and **BBC**.

	MBC	EBC	PBC	BBC
Structure of H_2 -lean form				
Structure of H_2 -rich form				
Melting points of H_2 -lean form ($^\circ\text{C}$)	154	187	200	198
Decomposition temperature of H_2 -lean form ($^\circ\text{C}$)	344	343	347	364
H_2 capacity (wt %)	5.86	5.67	5.49	5.31

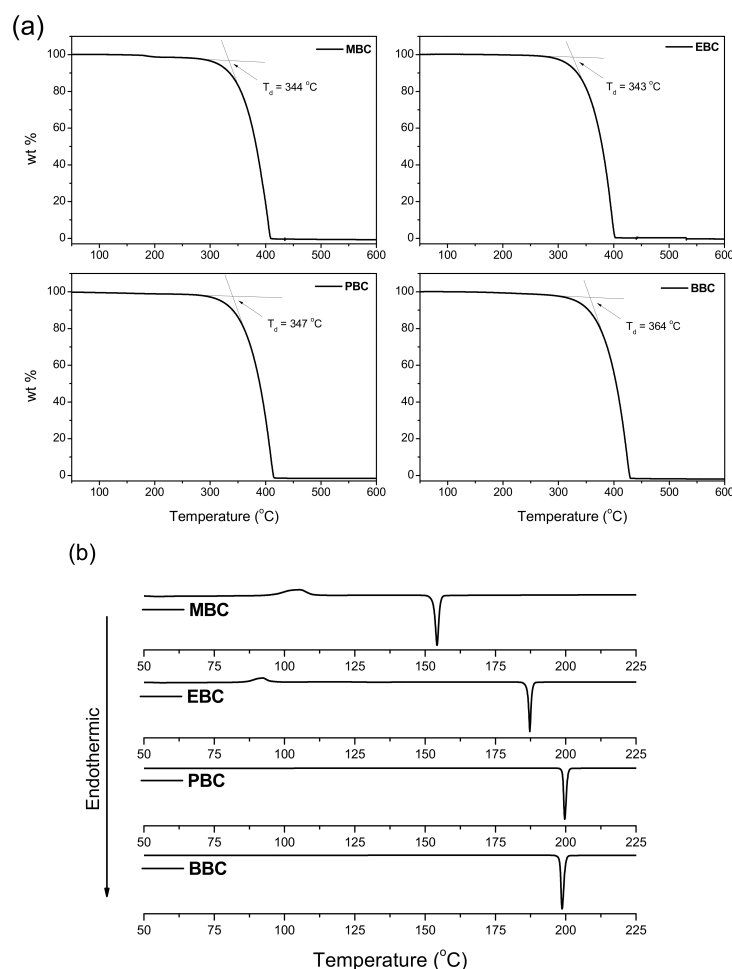


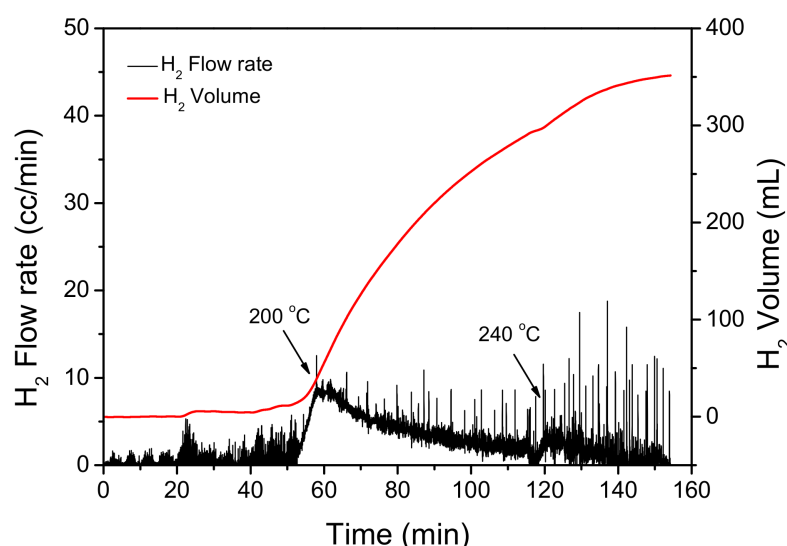
Figure 1. (a) Thermogravimetric analysis (TGA) and (b) differential scanning calorimetry (DSC) diagrams for **MBC**, **EBC**, **PBC**, and **BBC**.

Table 2. Catalytic hydrogenation of **MBC**, **EBC**, **PBC**, and **BBC**.

	Catalyst	Reaction Condition	Feed Catalyst (g)/LOHC (g)	Ideal wt %	Experimental wt %
MBC	Ru/Al ₂ O ₃	190 °C/24 h	0.30/3.00	5.86 wt % 0.187 g	5.92 ± 0.24 wt % 0.189 ± 0.008 g
EBC	Ru/Al ₂ O ₃	190 °C/24 h	0.30/3.01	5.67 wt % 0.181 g	5.81 ± 0.24 wt % 0.185 ± 0.008 g
PBC	Ru/Al ₂ O ₃	190 °C/24 h	0.30/3.01	5.49 wt % 0.174 g	5.34 ± 0.24 wt % 0.170 ± 0.008 g
BBC	Ru/Al ₂ O ₃	190 °C/24 h	0.42/4.25	5.31 wt % 0.254 g	5.61 ± 0.24 wt % 0.269 ± 0.008 g

3.4. Catalytic Dehydrogenation Reactions

To determine the optimal conditions for the dehydrogenation reaction, the optimum dehydrogenation temperature was determined by a temperature ramping test. Because the hydrogenation reaction rate of **EBC–H** was the highest, the temperature ramping test was typically performed using **EBC–H**. As shown in Figure 2, the ramping test showed that the dehydrogenation reaction temperature was greater than 200 °C.

**Figure 2.** Representative temperature ramping test for dehydrogenation of **EBC**.

The dehydrogenation reaction (I) was carried out at 240, 260, and 280 °C. Palladium on alumina catalyst was chosen because this catalyst is known to be the best catalyst for dehydrogenation for carbazole-based compounds [33]. When injecting a fully hydrogenated **EBC–H** sample at 240 °C, the rate of hydrogen release was 60 cc/min. As shown in Figure 3a, an exponential hydrogen release was observed within 20 min, and the rate of hydrogen release decreased after 20 min. After the evolution of hydrogen gas ceased, the mixture was analyzed by ¹H NMR. As shown in Figure S13, the generation of a significant number of peaks attributed to aromatic ring protons of carbazole was observed, but the peaks attributed to protons of cyclic alkanes were still observed between 0 and 3 ppm. This means **EBC–H** was not completely dehydrogenated at 240 °C. When the dehydrogenation reaction proceeded at 260 °C for 30 min, the hydrogen release rate was 100 cc/min. ¹H NMR spectra of the reaction residues showed that the intensities of aliphatic proton peaks at 0–3 ppm were significantly reduced, as shown in Figure S14. However, peaks attributed to protons of cyclic alkanes were still observed, indicating that the dehydrogenation reaction was not completed yet. Finally, the dehydrogenation reaction temperature was increased to 280 °C. At this temperature, the hydrogen atoms were exponentially released within

10 min and the hydrogen release rate was calculated to be 150 cc/min. ^1H NMR spectra of the reaction residues showed that the peaks attributed to the protons of cyclic alkanes at 0–3 ppm completely disappeared, and only peaks attributed to protons of the bridged alkyl chain were observed, as shown in Figure S15. According to the dehydrogenation method (I), it was confirmed that the rate of hydrogen release and the amount of hydrogen increased as the reaction temperature was increased.

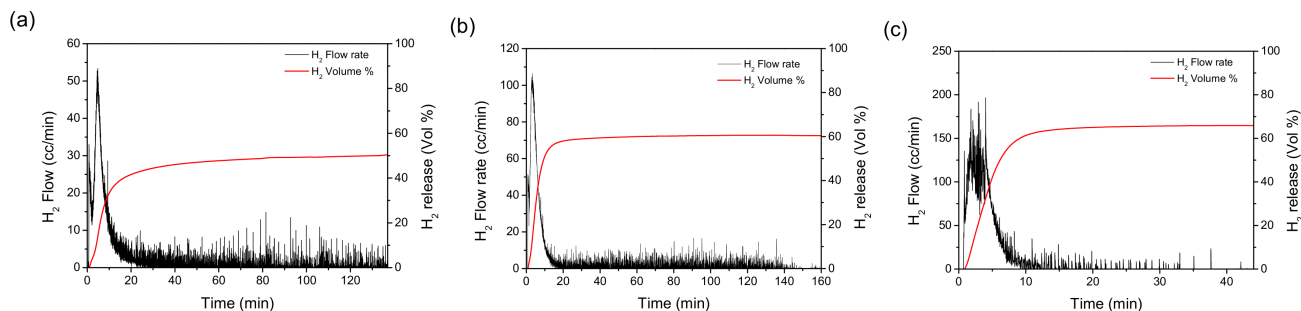


Figure 3. Dehydrogenation reaction kinetics of **EBC-H** at (a) 240, (b) 260, and (c) 280 °C.

Finally, the dehydrogenation method (II) was applied to confirm the complete dehydrogenation of all compounds at 280 °C. A fully hydrogenated sample and palladium on alumina were added to a flask and the reaction proceeded for 30 min at 280 °C. ^1H NMR spectra of the reaction residues showed that the aliphatic proton peaks between 0 and 3 ppm completely disappeared and only peaks attributed to the protons of the original carbazole aromatic rings were observed between 7 and 8 ppm, as shown in Figures S16–S18, indicating complete dehydrogenation of **MBC-H**, **PBC-H**, and **BBC-H**.

4. Conclusions

Four new compounds based on carbazole, **MBC**, **EBC**, **PBC**, and **BBC**, were designed and prepared to investigate their reactivity of hydrogen adsorption and desorption depending on the alkyl chain length. The gravimetric densities of **MBC**, **EBC**, **PBC**, and **BBC** were 5.86, 5.76, 5.49, and 5.39 H₂ wt %, respectively. The synthetic method for preparing these materials was optimized, and their chemical properties were characterized using ^1H and ^{13}C NMR spectrometry, mass spectrometry, and elemental analysis. All prepared materials had higher thermal stabilities than that of the reference material, **NEC**, which indicates that these materials are promising hydrogen storage materials for applications in fuel cell systems. The hydrogenation reactions were successfully demonstrated in a batch reactor with ruthenium on alumina as a catalyst at 190 °C within 24 h. Reversible reactions were also successfully demonstrated for all hydrogenated materials. Complete dehydrogenation reactions were demonstrated within 10 min in the presence of palladium on alumina as a catalyst at 280 °C. With the advantages of reversible hydrogenation and dehydrogenation reactions of **MBC/MBC-H**, **EBC/EBC-H**, **PBC/PBC-H**, and **BBC/BBC-H**, along with high thermal stabilities, it is anticipated that these materials are promising hydrogen storage materials for real applications in fuel cells. Among them, **EBC** would be the best material due to having the highest reaction rate and a relatively high gravimetric density.

Supplementary Materials: The following are available online at <https://www.mdpi.com/2073-4344/11/1/123/s1>, Figure S1: ^{13}C NMR of **MBC**; Figure S2: ^{13}C NMR of **EBC**; Figure S3: ^{13}C NMR of **PBC**; Figure S4: ^{13}C NMR of **BBC**; Figure S5: ^1H NMR of **MBC**; Figure S6: ^1H NMR of **EBC**; Figure S7: ^1H NMR of **PBC**; Figure S8: ^1H NMR of **BBC**; Figure S9: ^1H NMR after catalytic hydrogenation of **MBC**; Figure S10: ^1H NMR after catalytic hydrogenation of **EBC**; Figure S11: ^1H NMR after catalytic hydrogenation of **PBC**; Figure S12: ^1H NMR after catalytic hydrogenation of **BBC**; Figure S13: ^1H NMR of the resulting dehydrogenated products for **EBC-H** at 240 °C; Figure S14: ^1H NMR of the resulting dehydrogenated products for **EBC-H** at 260 °C; Figure S15: ^1H NMR of the resulting dehydrogenated products for **EBC-H** at 280 °C; Figure S16: ^1H NMR after catalytic dehydrogenation

of **MBC-H** at 280 °C; Figure S17: ¹H NMR after catalytic dehydrogenation of **PBC-H** at 280 °C; Figure S18: ¹H NMR after catalytic dehydrogenation of **BBC-H** at 280 °C.

Author Contributions: Conceptualization, synthesis, and characterization, J.J.; hydrogenation/dehydrogenation catalytic activity assay, B.S.S.; supervision, methodology, further data analysis and writing—review and editing, J.W.K. and W.-S.H. All authors have read and agreed to the published version of the manuscript.

Funding: This work was supported by the New & Renewable Energy Core Technology Program of the Korea Institute of Energy Technology Evaluation and Planning (KETEP), granted financial resource from the Ministry of Trade, Industry & Energy, Korea (No.20153030041030) and the National Research Foundation (NRF) funded by the Ministry of Science, Korea, ICP (2019M3E6A1103866).

Institutional Review Board Statement: Not applicable.

Informed Consent Statement: Not applicable.

Data Availability Statement: Data available in a publicly accessible repository.

Conflicts of Interest: The authors declare no conflict of interest.

References

1. Zou, H.; Guo, F.; Luo, M.; Yao, Q.; Lu, Z.-H. La(OH)₃-decorated NiFe nanoparticles as efficient catalyst for hydrogen evolution from hydrous hydrazine and hydrazine borane. *Int. J. Hydrog. Energy* **2020**, *45*, 11641–11650. [[CrossRef](#)]
2. Zhang, L.; Ji, L.; Yao, Z.; Yan, N.; Sun, Z.; Yang, X.; Zhu, X.; Hu, S.; Chen, L. Facile synthesized Fe nanosheets as superior active catalyst for hydrogen storage in MgH₂. *Int. J. Hydrog. Energy* **2019**, *44*, 21955–21964. [[CrossRef](#)]
3. Wan, C.; Cheng, D.-G.; Chen, F.; Zhan, X. Fabrication of CeO₂ nanotube supported Pt catalyst encapsulated with silica for high and stable performance. *Chem. Commun.* **2015**, *51*, 9785–9788. [[CrossRef](#)] [[PubMed](#)]
4. Muzzio, M.; Lin, H.; Wei, K.; Guo, X.; Yu, C.; Yom, T.; Xi, Z.; Yin, Z.; Sun, S. Efficient Hydrogen Generation from Ammonia Borane and Tandem Hydrogenation or Hydrodehalogenation over AuPd Nanoparticles. *ACS Sustain. Chem. Eng.* **2020**, *8*, 2814–2821. [[CrossRef](#)]
5. Zheng, J.; Liu, X.; Xu, P.; Liu, P.; Zhao, Y.; Yang, J. Development of high pressure gaseous hydrogen storage technologies. *Int. J. Hydrog. Energy* **2012**, *37*, 1048–1057. [[CrossRef](#)]
6. Sadaghiani, M.S.; Mehrpooya, M. Introducing and energy analysis of a novel cryogenic hydrogen liquefaction process configuration. *Int. J. Hydrog. Energy* **2017**, *42*, 6033–6050. [[CrossRef](#)]
7. Gleichweit, C.; Amende, M.; Bauer, U.; Schernich, S.; Höfert, O.; Lorenz, M.P.A.; Zhao, W.; Müller, M.; Koch, M.; Bachmann, P.; et al. Alkyl chain length-dependent surface reaction of dodecahydro-*N*-alkylcarbazoles on Pt model catalysts. *J. Chem. Phys.* **2014**, *140*, 204711. [[CrossRef](#)]
8. Makowski, P.; Thomas, A.; Kuhn, P.; Goettmann, F. Organic materials for hydrogenstorage applications: From physisorption on organic solids to chemisorption in organic molecules. *Energy Environ. Sci.* **2009**, *2*, 480–490. [[CrossRef](#)]
9. Cacciola, G.; Giordano, N.; Restuccia, G. Cyclohexane as a liquid phase carrier in hydrogen storage and transport. *Int. J. Hydrog. Energy* **1984**, *9*, 411–419. [[CrossRef](#)]
10. Maria, G.; Marin, A.; Wyss, C.; Muller, S.; Newson, E. Modelling and scaleup of the kinetics with deactivation of methylcyclohexane dehydrogenation for hydrogen energy storage. *Chem. Eng. Sci.* **1996**, *51*, 2891–2896. [[CrossRef](#)]
11. Pradhan, A.U.; Shukla, A.; Pande, J.V.; Karmarkar, S.; Biniwale, R.B. A feasibility analysis of hydrogen delivery system using liquid organic hydrides. *Int. J. Hydrog. Energy* **2011**, *36*, 680–688. [[CrossRef](#)]
12. Biniwale, R.B.; Rayalu, S.; Devotta, S.; Ichikawa, M. Chemical hydrides: A solution to high capacity hydrogen storage and supply. *Int. J. Hydrog. Energy* **2008**, *33*, 360–365. [[CrossRef](#)]
13. Alhumaidan, F.; Cresswell, D.; Garforth, A. Hydrogen storage in liquid organic hydride: Producing hydrogen catalytically from methylcyclohexane. *Energy Fuels* **2011**, *25*, 4217–4234. [[CrossRef](#)]
14. Crabtree, R.H. Hydrogen storage in liquid organic heterocycles. *Energy Environ. Sci.* **2008**, *1*, 134–138. [[CrossRef](#)]
15. Clot, E.; Eisenstein, O.; Crabtree, R.H. Computational structure—Activity relationships in H₂ storage: How placement of N atoms affects release temperatures in organic liquid storage materials. *Chem. Commun.* **2007**, *22*, 2231–2233. [[CrossRef](#)] [[PubMed](#)]
16. Eblagon, K.M.; Tam, K.; Yu, K.M.K.; Tsang, S.C.E. Comparative study of catalytic hydrogenation of 9-ethylcarbazole for hydrogen storage over noble metal surfaces. *J. Phys. Chem. C* **2012**, *116*, 7421–7429. [[CrossRef](#)]
17. Eblagon, K.M.; Tam, K.; Tsang, S.C.E. Comparison of catalytic performance of supported ruthenium and rhodium for hydrogenation of 9-ethylcarbazole for hydrogen storage applications. *Energy Environ. Sci.* **2012**, *5*, 8621–8630. [[CrossRef](#)]
18. Eblagon, K.M.; Tam, K.; Yu, K.M.K.; Zhao, S.-L.; Gong, X.-Q.; He, H.; Ye, L.; Wang, L.-C.; Ramirez-Cuesta, A.J.; Tsang, S.C. Study of catalytic sites on ruthenium for hydrogenation of *N*-ethylcarbazole: Implications of hydrogen storage via reversible catalytic hydrogenation. *J. Phys. Chem. C* **2010**, *114*, 9720–9730. [[CrossRef](#)]
19. Eblagon, K.M.; Rentsch, D.; Friedrichs, O.; Remhof, A.; Zuetzel, A.; Ramirez-Cuesta, A.J.; Tsang, S.C. Hydrogenation of 9-ethylcarbazole as a prototype of a liquid hydrogen carrier. *Int. J. Hydrog. Energy* **2010**, *35*, 11609–11621. [[CrossRef](#)]

20. Sotoodeh, F.; Smith, K.J. Analysis of H₂ release from organic polycyclics over Pd catalysts using DFT. *J. Phys. Chem. C* **2013**, *117*, 194–204. [[CrossRef](#)]
21. Sotoodeh, F.; Huber, B.J.M.; Smith, K.J. The effect of the N atom on the dehydrogenation of heterocycles used for hydrogen storage. *Appl. Catal. A Gen.* **2012**, *419*, 67–72. [[CrossRef](#)]
22. Sotoodeh, F.; Huber, B.J.M.; Smith, K.J. Dehydrogenation kinetics and catalysis of organic heteroaromatics for hydrogen storage. *Int. J. Hydrog. Energy* **2012**, *37*, 2715–2722. [[CrossRef](#)]
23. Sotoodeh, F.; Smith, K.J. Structure sensitivity of dodecahydro-*N*-ethylcarbazole dehydrogenation over Pd catalysts. *J. Catal.* **2011**, *279*, 36–47. [[CrossRef](#)]
24. Sotoodeh, F.; Smith, K.J. Kinetics of hydrogen uptake and release from heteroaromatic compounds for hydrogen storage. *Ind. Eng. Chem. Res.* **2010**, *49*, 1018–1026. [[CrossRef](#)]
25. Wang, Z.; Tonks, I.; Belli, J.; Jensen, C.M. Dehydrogenation of *N*-ethyl perhydrocarbazole catalyzed by PCP pincer iridium complexes: Evaluation of a homogenous hydrogen storage system. *J. Organomet. Chem.* **2009**, *694*, 2854–2857. [[CrossRef](#)]
26. Sotoodeh, F.; Zhao, L.; Smith, K.J. Kinetics of H₂ recovery from dodecahydro-*N*-ethylcarbazole over a supported Pd catalyst. *Appl. Catal. A Gen.* **2009**, *362*, 155–162. [[CrossRef](#)]
27. Preuster, P.; Fang, Q.; Peters, R.; Deja, R.; Nguyen, V.N.; Blum, L.; Stolten, D.; Wasserscheid, P. Solid oxide fuel cell operating on liquid organic hydrogen carrier-based hydrogen e making full use of heat integration potentials. *Int. J. Hydrog. Energy* **2018**, *43*, 1758–1768. [[CrossRef](#)]
28. Müller, K.; Thiele, S.; Wasserscheid, P. Evaluations of concepts for the integration of fuel cells in liquid organic hydrogen carrier systems. *Energy Fuels* **2019**, *33*, 10324–10330. [[CrossRef](#)]
29. Heublein, N.; Stelzner, M.; Sattelmayer, T. Hydrogen storage using liquid organic carriers: Equilibrium simulation and dehydrogenation reactor design. *Int. J. Hydrog. Energy* **2020**, *45*, 24902–24916. [[CrossRef](#)]
30. Brückner, N.; Obesser, K.; Bösmann, A.; Teichmann, D.; Arlt, W.; Dungs, J.; Wasserscheid, P. Evaluation of industrially applied heat-transfer fluids as liquid organic hydrogen carrier systems. *ChemSusChem* **2014**, *7*, 229–235. [[CrossRef](#)]
31. Sun, J.; Jiang, H.-J.; Zhang, J.-L.; Tao, Y.; Chen, R.-F. Synthesis and characterization of heteroatom substituted carbazole derivatives: Potential host materials for phosphorescent organic light-emitting diodes. *New J. Chem.* **2013**, *37*, 977–985. [[CrossRef](#)]
32. Ohta, H.; Tetsukawa, H.; Noto, N. Enantiotopically selective oxidation of α,ω -diols with enzyme systems of microorganisms. *J. Org. Chem.* **1982**, *47*, 2400–2404. [[CrossRef](#)]
33. Yang, M.; Dong, Y.; Fei, S.; Ke, S.; Cheng, H. A comparative study of catalytic dehydrogenation of perhydro-*N*-ethylcarbazole over noble metalcatalys. *Int. J. Hydrog. Energy* **2014**, *39*, 18976–18983. [[CrossRef](#)]